



Hrvatsko društvo za kontrolu bez razaranja
Croatian Society of NDT

International Conference
on Non-Destructive Testing

MATEST 2011

Under the auspices of: / Pokrovitelji:

EF European Federation for
Non-Destructive Testing
NDT

Faculty of Electrical Engineering, Mechanical
Engineering and Naval Architecture, Split



Fakultet elektrotehničke, strojarstva
i brodogradnje, Split

University of Split



Sveučilište u Splitu

The County of Split - Dalmatia



Špišićka - Jadranska laganija



HAA

Hrvatska akreditacijska agencija
Croatian Accreditation Agency



HZN

Hrvatski zavod za norme
Croatian Standards Institute

Sponsor / Sponzor:



imagination at work.

ABSTRACT BOOK

Editor: Nikša KRNIĆ, Ph. D. Assoc. Prof.



CROATIA, SPLIT

2nd - 5th November 2011

Hotel Le Meridien



MATEST 2011

International Conference on Non-Destructive Testing

Abstracts are published in alphabetical order of the first author surname.

CONTENT:

Page:

1. AUFRICHT G., BALAS G., sen.:
MODULAR CERTIFICATION ACCORDING to EN 473, EN 4179, NAS 410 and UIC
KODEX 960V 6
2. BAJZEK BREZAK B., VREBČEVIĆ M., MUCKO V.:
ACREDITATION in the FIELD of NDT and WELDING 7
- 3 CARBONI M: A NEW PERSPECTIVE for the INTERPRETATION of ULTRASONIC
RESPONSES and its CONSEQUENCES in the DETERMINATION of „PROBABILITY
of DETECTION“ CURVES 8
4. CVITANOVIĆ M., NADINIĆ B., NICHEV V., CETVERIKOV A., RAZIGRAEV N.,
RAZIGRAEV A.: OVERVIEW of NON-DESTRUCTIVE TESTING SYSTEMS
QUALIFICATION for WWER 1000 NUCLEAR POWER PLANTS 9
5. ČUČIĆ V., SEDLAR D., LOZINA Ž: IDENTIFICATION of MECHANICAL SYSTEM
for NDT 10
6. FINC M., GRUM J.: USE of THERMOGRAPHY for the EVALUATION of FORGED
WIRE CONNECTION QUALITY 11
7. FÜCSÖK F.: INTERLABORATORY NON-DESTRUCTIVE TESTS – ROLE and
ACHIEVEMENTS of HUNGARIAN ASSOCIATION for NDT 12
8. IVKOVIĆ Z., LOLIĆ S.: RELIABILITY of NON-DESTRUCTIVE TESTING
RESULTS of WELDED JOINTS APPLICATION of SURFACE NDT METHODS for
UNDERWATER INSPECTION 13
9. KAZAKEVYCH M.L.: APPLICATION of SURFACE NDT METHODS for
UNDERWATER INSPECTION 14
10. KOVÁČIK M., KUČIK P.: ULTRASONIC TESTING of THICK WALL WELDED
JOINTS 15
11. KRNIĆ N.: NON-DESTRUCTIVE TESTING in SHIPBUILDING and for
OFFSHORE and UNDERWATER APPLICATIONS 16

A NEW PERSPECTIVE for the INTERPRETATION of ULTRASONIC RESPONSES and its CONSEQUENCES in the DETERMINATION of „PROBABILITY of DETECTION“ CURVES

Michele, **CARBONI**, *DEPARTMENT of MECHANICAL ENGINEERING, POLITECNICO DI MILANO, Milano, ITALY*, Contacts – Phone: +39-02-23998253; e-mail: michele.carboni@polimi.it

ABSTRACT - *One of the most important aspects in the application of the „Damage Tolerant“ design approach to mechanical components is the probability to detect possible in-service defects.*

In the present paper, a novel approach, recently proposed by the author, to the interpretation of ultrasonic responses is presented. Such approach allows a new way of thinking for a more flexible and versatile procedure for the derivation of „probability of detection“ curves. A high number of dedicated UT inspection experiments, carried out on artificial and natural fatigue cracks, are described in order to build up the procedure with the appropriate statistical parameters. Since the experiments typically needed to derive probability of detection curves with proper statistical reliability are expensive, the possibility to exchange part of the experiments with suitable numerical simulation is here considered.

1. INTRODUCTION

Considering components subjected to fatigue, it is licit to expect crack initiation and consequent propagation during service. To face this problem, it is possible to employ the “Damage Tolerant” design approach whose philosophy consists ([1,2]) in determining the most opportune in-service inspection interval given the “Probability of Detection” (POD) curve ([3-5]) of the adopted “Non-Destructive Testing” (NDT) method or, alternatively, in defining the needed NDT specifications given a programmed inspection interval. Structural integrity of safety components during service is then strictly related to the following factors ([1-2]): i) the performance and the reliability of the adopted NDT procedure; ii) the crack propagation behavior of the adopted material; iii) the influence of the geometry of the cracked body on the crack driving force; iv) the reliable knowledge of service loads.

The present research is focused, between the just described points, on NDT effectiveness which is directly related to the reliable knowledge of the POD curve of the adopted inspection method. Traditionally, such probabilities are explicitly expressed and plotted in terms of a characteristic linear dimension of defects (depth, length, diameter, ...). However, they are also a function of many other physical and operative factors such as: the adopted NDT method, the material, geometry, defect type, instrumentation, human and environmental effects. This means that very rarely the

POD curve derived for a given configuration can be used for other configurations, even if similar. Another critical aspect of POD curves is the need, for reliability and design, of a statistical characterisation of the largest defect that can be missed and not the smallest defect that can be observed. For this reason, POD curves should always be provided together with a suitable lower confidence limit (typically 95%) which needs a lot of experimental results to be achieved.

Considering, here, the specific case of ultrasonic (UT) NDT applied to railway axles (even if the approach is generally applicable to every UT inspection of mechanical components), a novel approach, recently proposed by the author [6], to the interpretation of UT responses is firstly built up and presented by means of a very high number of experimental responses coming from artificial and natural defects. Since experiments are expensive, it is then investigated the possibility to apply the "model-assisted probability of detection" (MAPOD) approach [7-9] which is very recent (the first publications come from 2003) and it is based on the idea to substitute part of the experimental responses with numerical ones obtained from suitable physical models. However, it is worth remembering that MAPOD does not allow to eliminate all the experimental activity because not all the relevant parameters are controlled by well-known physical models.

2. THE "REFLECTING AREA" APPROACH

The considered material is an A4T steel grade typically used for the production of railway axles and characterised by a longitudinal wave speed $V_L=5920$ m/s and a shear wave speed $V_T=3230$ m/s. All the experimental tests were carried out by the same operator using a Gilardoni RDG500 defectoscope equipped with a ATM45/4 single 8x9 mm crystal probe. The UT response of the inspected defects was always recorded at a gain level equal to 48 dB, corresponding to the response echo of a big reflector (observed in a first leg configuration) set to the 80% of the display. The piece-probe coupling was guaranteed by means of grease and suitable Plexiglas wedges.

Twenty artificial defects were realised on the external surface of six chunks cut from axles made of A4T (Fig. 1a). Particularly, such defects are characterised by (Fig. 1b): different geometries (saw-cut, convex, concave), different dimensions (depths from 0.5 mm to 8 mm) and different manufacturing processes (traditional machining, EDM). All the defects could be inspected adopting both a 1st leg inspection configuration (direct reflection on the defect) and a 2nd leg one (with an intermediate reflection on the bore). It is important to remark that the industrial UT inspection of hollow axles is carried out only in a 1st leg configuration by means of dedicated bore-probes.

UT responses of artificial defects are reported in Figure 2a in terms of the traditional linear dimension of the defect (in this case, the depth). As it can be seen, the standard deviation is so high that the response coming from two different times of flight (one double of the other) intersect. This could be attributed [6] to the influence that the defect shape has on the UT response of defect having the same depth, but different morphology.

In order to eliminate the influence of the morphology of the defect, it was then proposed [6] to plot UT responses in terms of the reflecting area of defects, i.e. the intersection between the area of the sound beam at the considered time of flight and

the area of the defect itself. More details on the procedure can be found in [6]. Results are reported in Figure 2b, where the influence of the morphology on UT responses (and, consequently, the standard deviation) is evidently decreased.

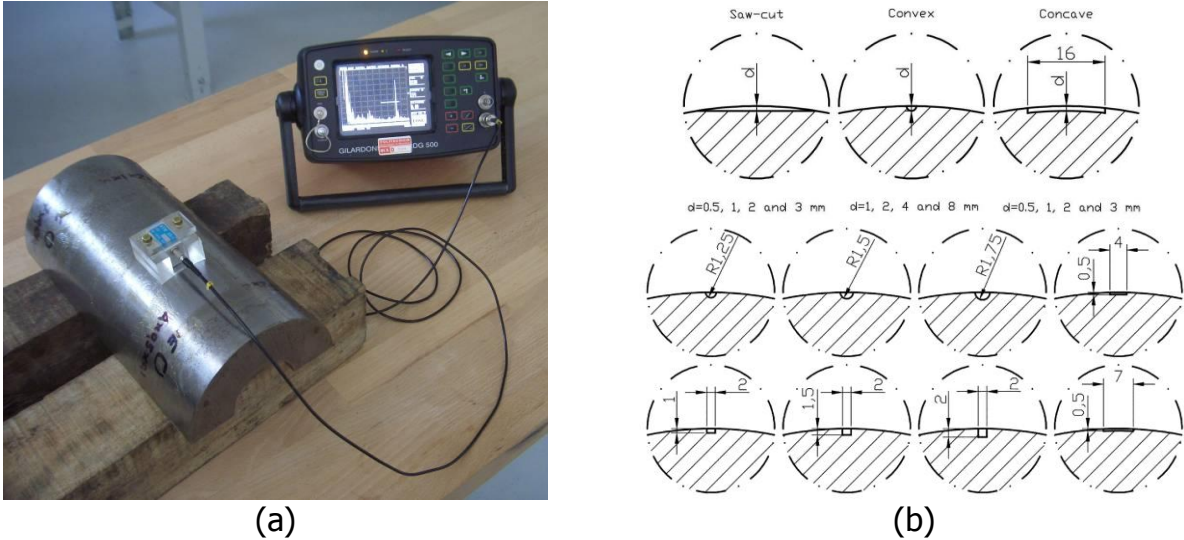


Figure 1 UT inspection of different artificial defects

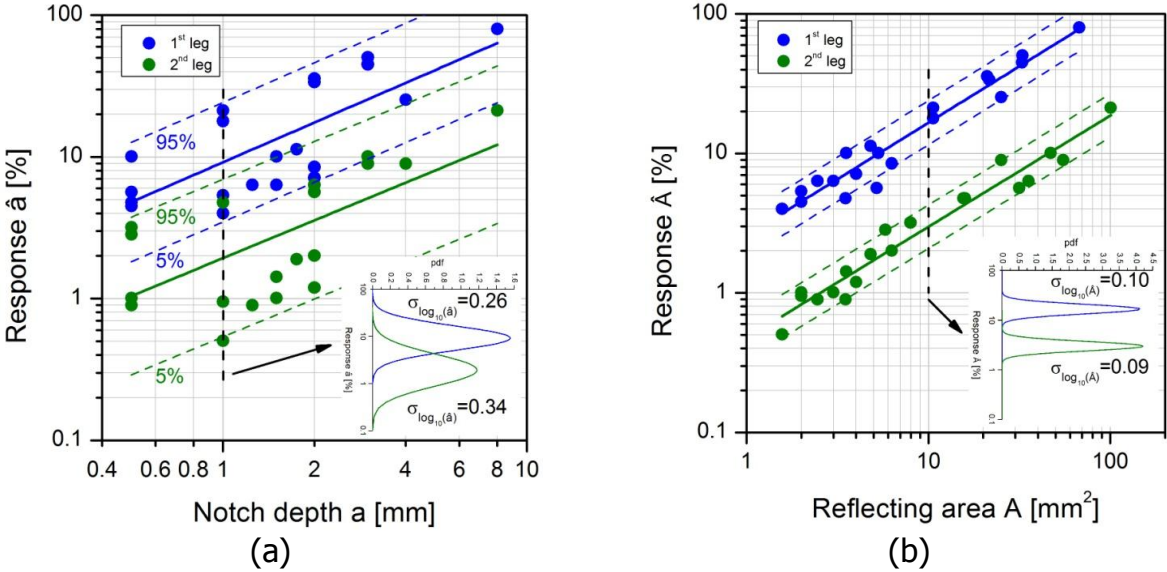


Figure 2 Comparison between UT responses in terms of (a) depth and (b) reflecting area

UT inspections were then carried out on natural fatigue cracks induced, by means of proper artificial micro-defects, in the body of three full-scale axles (Fig. 3a) made of A4T and fatigue tested by the dedicated facility available at the Dept. of Mechanical Engineering of Politecnico di Milano. Since the loading condition of axles on the bench can be assimilated to a three point rotating bending, the shape of natural fatigue cracks is expected to be similar to the convex artificial defects shown in Figure 2b, i.e. semi-elliptical or semi-circular. Inspections were carried out during crack propagation tests so having the possibility to measure evolving cracks changing their dimensions with the increasing number of cycles. In this case, inspections could only be carried out considering the 2nd leg configuration.

The obtained results are shown in Figures 3b and 3c in terms of depth and reflecting area, respectively. As expected, it is possible a saturation level above which cracks and

defects can be assimilated to big reflectors. In the case of depth, the behaviour of fatigue cracks is very different from that of artificial defects, as often reported in the literature [10]. Considering, instead, the reflecting area, the correlation seems to get much better, suggesting that the reflecting properties of a natural fatigue crack are similar to that of artificial defects (this conclusion cannot be generalised to other kinds of natural cracks).

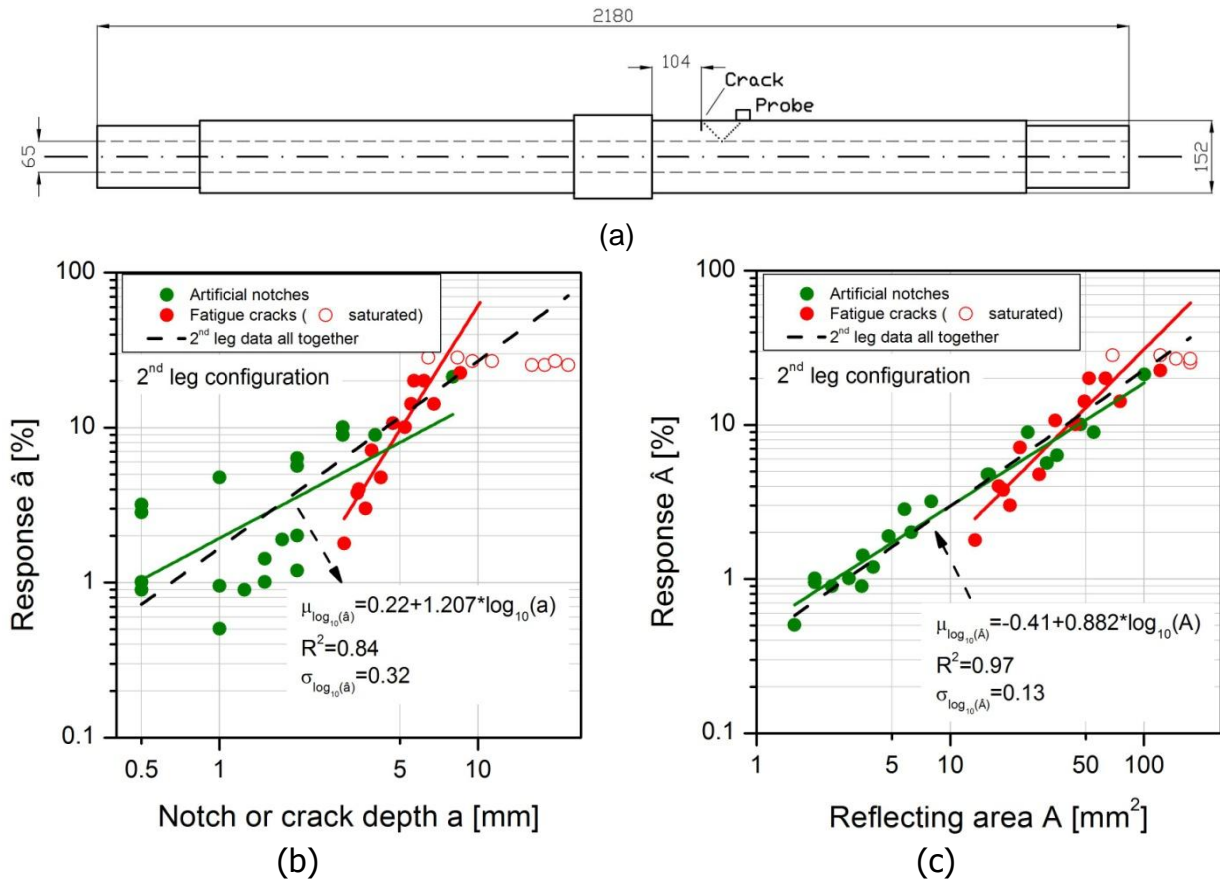


Figure 3 UT responses of natural fatigue cracks: a) full-scale axle; b) results in terms of depth; c) results in terms of reflecting area

3. NUMERICAL SIMULATIONS FOR POD CURVES

The obtainment of the results described in the previous section required a big experimental effort in terms of time and costs. This problem of deriving POD curves is well known in the NDT community, so, recently, cheaper methods alternative to the empirical one are being researched and MAPOD is one of those. Particularly, POD curves are based on the statistical distribution of defect responses which, on the other hand, are controlled by a number of factors related to the details of the adopted NDT procedure. Today, the effects of many of these factors can be simulated by proper numerical models and MAPOD takes the maximum advantage of this possibility. Unfortunately, as already stated in the Introduction, MAPOD does not allow to eliminate all the experiments because today not all of the factors can be described by known physical models. It is also important to remark that MAPOD can be applied to every NDT technique, not only to UT considered in the present research.

At the moment, two different MAPOD variations (Fig. 4) are reported in the literature [8], but, in the future, it is possible that they will become two interpretations of the same process. The first variation is called "transfer function" (Fig. 4a) because it suggests to use numerical models in order to ease the transferability of POD curves obtained in a given condition to other conditions where some parameters are changed. The second variation, called "complete MAPOD" (Fig. 4b), foresees a minimum set of experiments in order to characterise those inspection factors not described by known physical models together with numerical simulations for all the other factors.

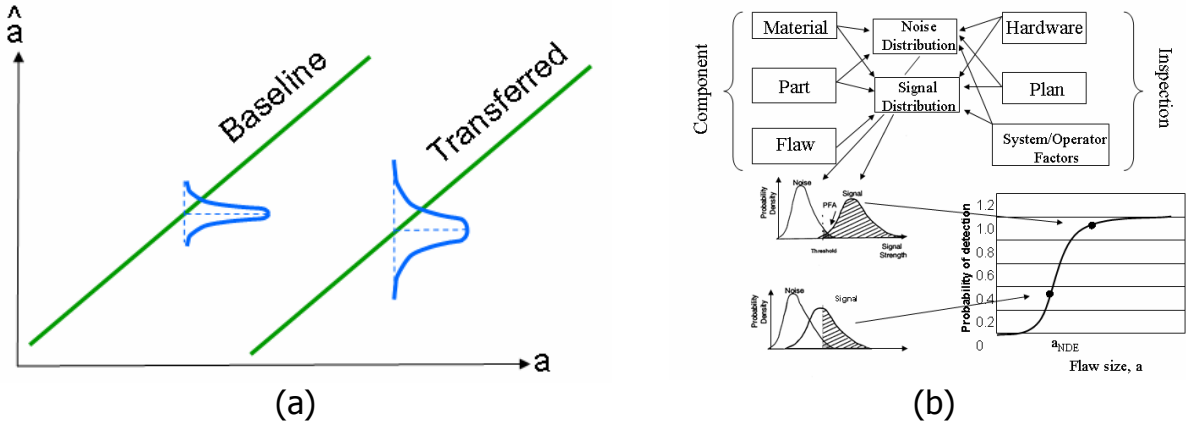


Figure 4 Two MAPOD approaches [8]: a) transfer function; b) complete approach

Both MAPOD variations can be successfully applied to the UT inspection of railway axles. In the present research, numerical simulations are carried out by means of the CIVA 10.0b dedicated software package [11], able to simulate UT, ET and RT inspections. First of all, the calibration of the numerical model (Fig. 5a) was carried out simulating the 2nd leg inspection of the convex artificial defect having radius equal to 8 mm and consisted in looking for and setting the numerical gain able to yield an A-Scan height equal to the experimental one.

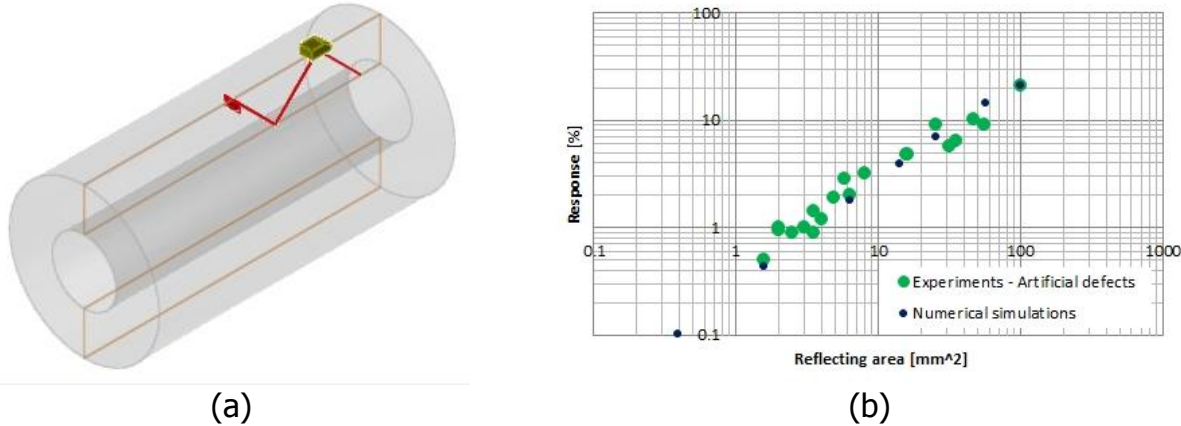


Figure 5 Calibration of the numerical model: a) numerical set-up; b) comparison between 2nd leg experiments and numerical results

Keeping the numerical gain constant, a series of convex semi-circular defects with increasing reflecting area (radius from 0.5 mm to 8 mm) was then simulated and the results are shown in Figure 5b. As it can be seen, numerical responses are very well aligned with the experiments, suggesting the exactness of the calibration and the correct set-up of the numerical model for the following analyses.

3.1. "TRANSFER FUNCTION" APPROACH

As an applicative example of the "transfer function" approach, the calibrated numerical model was used in order to simulate the UT response of the same convex defects used for the calibration, but, in this case, inspected in the 1st leg configuration. In this way: i) a condition similar to the calibration is considered but with one significantly different factor (the time of flight); ii) the experimental responses in 1st leg are available to validate the numerical results. The numerical set-up is shown in Figure 6a where the only differences with the calibration set-up are the location of the probe (inside the bore) and the shape of the Plexiglas wedge (from concave to convex). All the other factors were unchanged, included the numerical gain determined during the calibration. The comparison between numerical results and experimental data is shown in Figure 6b. As it can be seen, numerical simulations are very well aligned with experiments: this result suggests that, in absence of experimental data, the model could allow to determine the POD curve of 1st leg inspections starting from the experimental calibration of defect inspected in 2nd leg configuration.

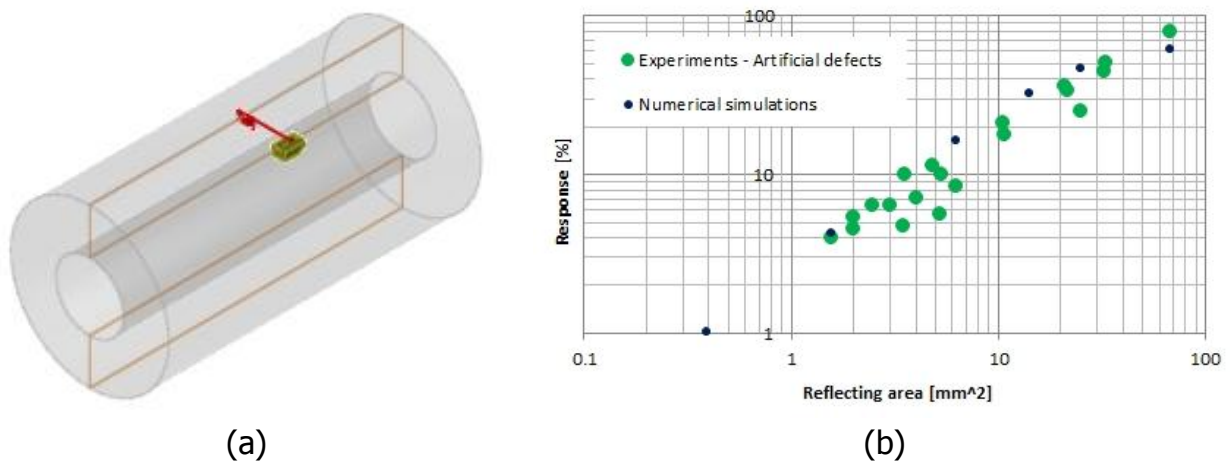


Figure 6 Application of the "transfer function" approach: a) numerical set-up; b) comparison between 1st leg experiments and numerical results

3.2. "COMPLETE MAPOD" APPROACH

The numerical results shown in Figures 5b and 6b are surely useful, interesting and represent a first effective MAPOD tool to evaluate the performance of the considered inspection methodology. Unfortunately, they do not provide information about the intrinsic variability of experimental results (as it is evident from the significantly different standard deviations between experiments and simulations) because they are obtained considering "ideal" conditions where, for example, the coupling is perfect, the probe position is exactly the one maximising the response, etc. The consequence is that the confidence band of numerical results is an artifice and absolutely not representative of the one of experimental data (see Section 4).

In the necessity to characterise also the confidence of POD curves, the application of the "complete MAPOD" approach suggests to model, during simulations, every source of variability of the NDT response by means of a suitable statistical distribution. It is worth remarking again that not all the sources of variability are today describable by an effective statistical model.

For simplicity and with a demonstration aim, a single source of variability is here considered: the position of the probe along the longitudinal axis of the axle with respect to the condition of maximum response of the defect inspected in 2nd leg configuration (Fig. 7a). The analysis is based on the Monte Carlo method: before any numerical run, a value of the longitudinal position of the probe, with respect to the defect, is randomly extracted from a normal distribution having mean equal to the position of the defect maximization and coefficient of variation CV=0.1. It is important to add that such distribution was assumed but not experimentally verified and it should represent the fact that, during the automatic inspection of axles, the advancement of the probe is in discrete steps, so that rarely the probe is located in the best position. Five defects having R=0.5, 1, 2, 4 and 8 mm were considered and for each of them thirty numerical runs were carried out so totalising 150 runs. This number of analyses for each defect was so chosen because the minimum number of data, for a given defect, needed for the definition of the 95% confidence band is 29. Figure 7b shows the obtained results.

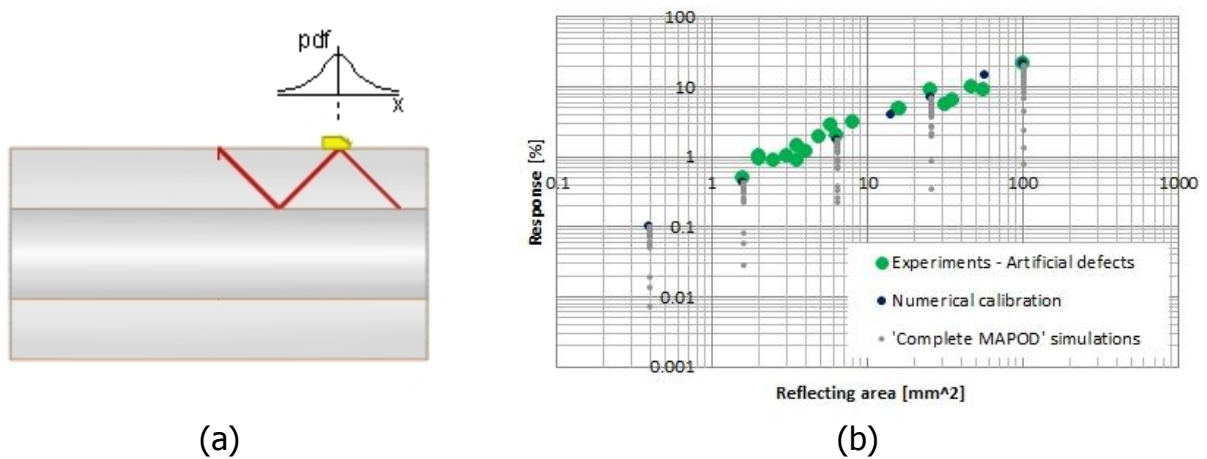


Figure 7 Application of the "complete MAPOD" approach: a) model definition; b) comparison between 2nd leg experiments and numerical results

The best performance, i.e. the highest numerical responses, corresponds to the calibration points since they were obtained positioning the probe in the maximising location. For all the other numerical results, the response is lower because the sound beam does not impact the defect in the best way. Generally, the numerical standard deviation seems to be significant and is spread on about a decade of the responses.

It is, finally, worth remarking that more complex numerical results based on more sources of variability can be achieved generalising the described procedure: before a numerical run, a value must be extracted from each of the statistical distributions representing the each of the considered sources of variability.

4. DERIVATION OF POD CURVES

Signal response (\hat{A} vs. A , where \hat{A} is the response obtained from the defect having reflecting area equal to A [4]) data were mathematically characterized applying a normal statistical model [3] based, on a bi-logarithmic plot, on a linear trend of the mean $\mu_{\log_{10}(\hat{A})}$ with flaw dimension and a constant standard deviation $\sigma_{\log_{10}(\hat{A})}$:

$$\begin{cases} \mu_{\log_{10}(\hat{A})} = \beta_0 + \beta_1 \cdot \log_{10}(A) \\ \sigma_{\log_{10}(\hat{A})} = \beta_2 \end{cases} \quad (1)$$

where the parameters β_0 , β_1 and β_2 were determined interpolating data by means of the maximum likelihood method.

Generally, considering signal response data, a defect is regarded as “detected”, if \hat{A} exceeds some pre-defined “decision threshold” \hat{A}_{th} corresponding to the response of the defect to be detected with 50% probability ([3-5]). The POD curve can then be built, for each flaw dimension, calculating the probability of a given defect responding with an energy higher than the chosen threshold [3]:

$$POD(A) = \Pr[\log_{10}(\hat{A}) > \log_{10}(\hat{A}_{th})] \quad (2)$$

which can be written as:

$$POD(A) = 1 - F \left\{ \frac{\log_{10}(\hat{A}_{th}) - [\beta_0 + \beta_1 \cdot \log_{10}(A)]}{\beta_2} \right\} = F \left\{ \frac{\log_{10}(A) - \left[\frac{\log_{10}(\hat{A}_{th}) - \beta_0}{\beta_1} \right]}{\frac{\beta_2}{\beta_1}} \right\} \quad (3)$$

Eq. (3) represents the cumulative log-normal distribution characterized by the following mean μ and standard deviation σ :

$$\mu = \frac{\log_{10}(\hat{a}_{th}) - \beta_0}{\beta_1} \quad (4)$$

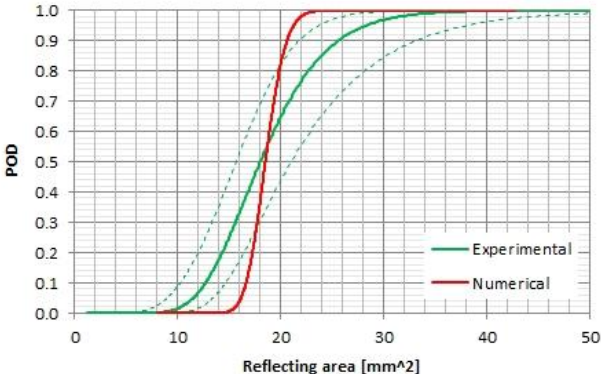
$$\sigma = \frac{\beta_2}{\beta_1} \quad (4')$$

where the β parameters are those previously derived. It is also evident that the choice of the decision threshold can be particularly critical on the achieved POD curves. The analysis of the effects of this choice is beyond the aims of the present research, so the following analyses are based on the response of the saw-cut having depth equal to 1 mm, one of the most traditional calibration defects for railway axles.

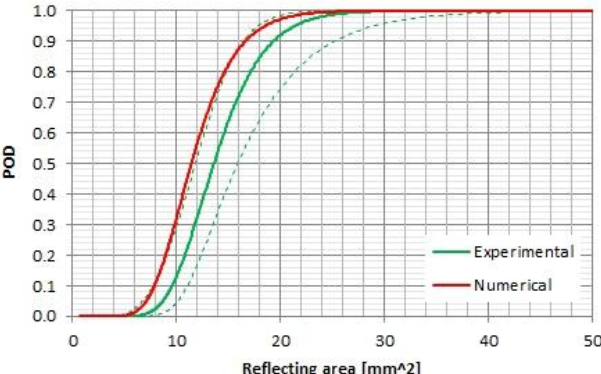
Figure 8a shows the comparison of the POD curves obtained from the artificial defects inspected in 2nd leg configuration and the calibration numerical results. No confidence bounds are reported for the numerical results due too few considered data. As it can be seen, the comparison is very satisfying because the numerical POD curve falls inside the 95% confidence interval of the experimental one so making the numerical results statistically indiscernible. The steeper slope of the numerical POD curve can be ascribed to the significantly lower standard deviation due to the reasons already explained in Section 3.2.

The same comments can be done observing Figure 8b which shows the comparison between the experimental POD for the artificial defects inspected in 1st leg configuration and the numerical simulation of the same defects using the “transfer function” approach: the numerical curve seems to coincide with the lower confidence limit of the

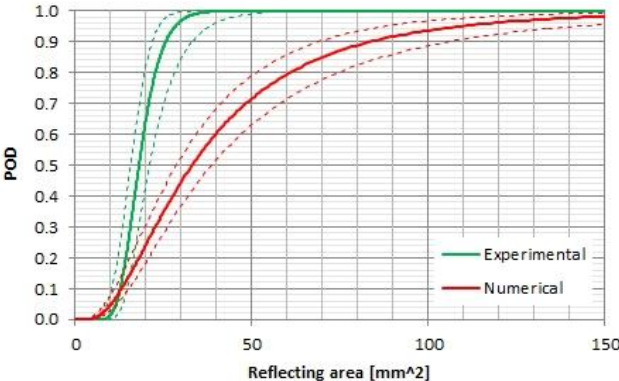
experimental data, suggesting again the statistical identity of the POD. Moreover, in this case, the standard deviation of numerical results is higher than in the previous analysis, so that the slope of the curve is more or less the same of the experimental POD curve.



(a)



(b)



(c)

Figure 8 POD curves: calibration; b) transfer function; c) complete MAPOD

Finally, Figure 8c shows the comparison between the experimental and the numerical data considered in the “complete MAPOD” approach. The mean trend of these two kind of data is different (numerical data parallel and lower than the experimental one) and this can explain why the 50% defect of the numerical POD curve is moved versus bigger reflecting areas. Moreover, the standard deviation of numerical data is bigger than that of experimental one, so explaining the less steep trend of the numerical POD curve.

5. CONCLUDING REMARKS

After a short summary of the “reflecting area” approach recently proposed by the author for a more effective interpretation of UT responses, the application of the MAPOD approach, based on the numerical modelling of the phenomenon, was presented together with its usefulness especially considering the possibility to lower the number of experiments needed to define POD curves. The obtained results seem to be very encouraging considering both the “transfer function” approach and the “complete MAPOD” one. In both cases, it was possible to obtain a good correspondence between experimental evidences and numerical results of UT inspection of railway axles, but more research is needed since the novelty of this modelling methodology.

6. REFERENCES

- [1] Zerbst U, Vormwald M., Andersch C., Mädler K and Pfuff M. The development of a damage tolerance concept for railway components and its demonstration for a railway axle. *Eng. Fract. Mech.* 2003;72:209-239.
- [2] Grandt AF Jr. *Fundamentals of structural integrity.* John Wiley & Sons Inc., Hoboken, 2003.
- [3] Georgiou GA. *Probability of Detection (POD) curves: derivation, applications and limitations.* Research Report 454, HSE Books, Health and Safety, Executive, UK, 2006.
- [4] ASM. *ASM handbook – Vol. 17: Non-destructive evaluation and quality control.* 1997.
- [5] MIL-HDBK-1823A. *Nondestructive evaluation system reliability assessment.* Department of Defense of the US, 2009.
- [6] M. Carboni. *A critical analysis of ultrasonic echoes coming from natural and artificial flaws and its implications in the derivation of probability of detection curves.* Submitted for publication to *NDT&E International*, 2011.
- [7] <http://www.cnde.iastate.edu/MAPOD/index.htm>.
- [8] R.B. Thompson, L. Brasche, J. Knopp, J. Malas, ‘Use of physics-based models of inspection processes to assist in determining probability of detection’, *Atti Aging Aircraft Conference*, 2006.
- [9] J.S. Knopp, J.C. Aldrin, E. Lindgren, C. Annis, ‘Investigation of a model-assisted approach to probability of detection evaluation’, *AFRL-ML-WP-TP-2006-494 Report*, AIR FORCE RESEARCH LABORATORY, 2006.
- [10] J.R. Birchack, C.G. Gardner, ‘Comparative ultrasonic response of machined slots and fatigue cracks in 7075 aluminum’, *Materials Evaluation* 1976;34(12):275-280.
- [11] CEA/CEDRAT, *CIVA 10.0b User’s Manual*, 2011.